Brain Topography (2021) 34:192–206
https://doi.org/10.1007/s10548-020-00815-z

ORIGINAL PAPER

Characterization of Source-Localized EEG Activity During Sustained Deep-Tissue Pain

Juan Manuel Völker[1] · Federico Gabriel Arguissain[1] · José Biurrun Manresa[1,2] · Ole Kæseler Andersen[1]

Received: 22 April 2020 / Accepted: 16 December 2020 / Published online: 5 January 2021

Abstract

Musculoskeletal pain is a clinical condition that is characterized by ongoing pain and discomfort in the deep tissues such as muscle, bones, ligaments, nerves, and tendons. In the last decades, it was subject to extensive research due to its high prevalence. Still, a quantitative description of the electrical brain activity during musculoskeletal pain is lacking. This study aimed to characterize intracranial current source density (CSD) estimations during sustained deep-tissue experimental pain. Twenty-three healthy volunteers received three types of tonic stimuli for three minutes each: computer-controlled cuff pressure (1) below pain threshold (*sustained deep-tissue no-pain*, SDTnP), (2) above pain threshold (*sustained deep-tissue pain*, SDTP) and (3) vibrotactile stimulation (VT). The CSD in response to these stimuli was calculated in seven regions of interest (ROIs) likely involved in pain processing: contralateral anterior cingulate cortex, contralateral primary somatosensory cortex, bilateral anterior insula, contralateral dorsolateral prefrontal cortex, posterior parietal cortex and contralateral premotor cortex. Results showed that participants exhibited an overall increase in spectral power during SDTP in all seven ROIs compared to both SDTnP and VT, likely reflecting the differences in the salience of these stimuli. Moreover, we observed a difference is CSD due to the type of stimulus, likely reflecting somatosensory discrimination of stimulus intensity. These results describe the different contributions of neural oscillations within these brain regions in the processing of sustained deep-tissue pain.

Keywords Tonic pain · EEG · Source localization · Cuff algometry · Muscle

Introduction

Musculoskeletal pain is a major health problem, and research into the underlying neurophysiological mechanisms is required to improve its understanding and management (Arendt-Nielsen et al. 2011). It is a clinical condition that is characterized by ongoing pain and discomfort in the deep tissues such as muscle, bones, ligaments, nerves and tendons (Kehl and Fairbank 2003; Arendt-Nielsen et al. 2011). Clinical musculoskeletal pain is usually not a short-lasting and time-bound sensation; even acute pain can last from minutes to days or weeks. In this regard, tonic rather than phasic experimental pain models better resemble clinical musculoskeletal pain (Svensson and Arendt-Nielsen 1995). Although many surrogate models can closely mimic musculoskeletal pain (e.g. injections of saline solution or nerve growth factor), they are invasive, and the time course and intensity of pain are hard to control. In this regard, recent developments in cuff pressure algometry allow for a non-invasive, more controllable setup (Polianskis et al. 2001).

People who suffer from musculoskeletal pain describe it as a sustained, intense and prolonged sensation (Soares and Jablonska 2004), all of which emphasize the disruptive ability of a painful stimulus to capture attention even without behavioural relevance and voluntary effort (Eccleston and Crombez 1999). Thus, pain has the intrinsic attribute of maintaining its salience over the duration of the stimulus,

Handling Editor: Hisao Nishijo.

✉ Juan Manuel Völker
jmv@hst.aau.dk

[1] Department of Health Science and Technology, Integrative Neuroscience Group, Center for Neuroplasticity and Pain (CNAP), Aalborg University, Aalborg, Denmark

[2] Institute for Research and Development in Bioengineering and Bioinformatics (IBB), CONICET-UNER, Oro Verde, Argentina

and it has been shown that the anterior insula (AI) and the anterior cingulate cortex (ACC) display sustained responses during painful transcutaneous electrical stimulation (Downar et al. 2003). These two brain regions are often activated together and are involved in detecting and filtering salient stimuli that are behaviorally relevant (Legrain et al. 2011). Since sustained deep-tissue pain can remain salient for a prolonged period, describing the activity of these regions may provide new insights into musculoskeletal pain mechanisms.

Previous studies that employed brain neuroimaging techniques such functional magnetic resonance (fMRI) and positron emission tomography (PET), have found that musculoskeletal pain is characterized by brain activation in numerous areas (Duerden and Albanese 2013). Among these regions, the primary somatosensory cortex (S1), the anterior insula (AI) and ACC are consistently reported in the literature as being involved in musculoskeletal pain (Kupers et al. 2004; Thunberg et al. 2005; Kim et al. 2013). Still, fMRI or PET are not suitable to assess neural oscillations with frequencies higher than 4 Hz (Ritter and Villringer 2006). On the contrary, techniques with high temporal resolution such as electroencephalography (EEG) or magnetoencephalography (MEG) provide a better measurement of neural oscillations, which are known to be in the range of 0.01 Hz to 100 Hz, and even higher (Cohen 2017). This characteristic makes EEG an invaluable tool to assess the neural dynamics during tonic pain (Ploner et al. 2017).

An important limitation of scalp EEG is that it does not provide direct information about the spatial localization of the underlying sources within the brain, because the electrodes record the superpositions of brain signals originating from the entire cortical grey matter. In this regard, there is a considerable number of inverse solution algorithms that allow estimating the active neuronal populations inside the brain, yet with limited precision (Michel et al. 2004; Michel and Murray 2012). Previous studies have characterized the neural correlates of superficial tonic painful stimulation using these techniques (Chang et al. 2002; Hansen et al. 2017). However, EEG studies that characterize brain response at the source level during sustained deep-tissue pain are scarce.

The main goal of this study was to characterize the current source density (CSD) estimations of brain source oscillations in healthy subjects during tonic, deep-tissue painful and non-painful mechanical pressure stimulation (Le Pera et al. 2000; Lavigne et al. 2004). It was hypothesized that sustained deep-tissue pain would result in increased power of neural oscillations compared to non-painful stimulation, reflecting higher activity in regions involved in pain processing.

Materials and Methods

Subjects

Twenty-three healthy human subjects (nine males, fourteen females, mean ± SD age: 24.5 ± 2.5 years) participated in the study. The participants were recruited by advertisement at the local university. None of the participants suffered from chronic pain, had any pain or used pain medication during one week before participation. Written informed consent was obtained from every participant. This study was approved by the ethics committee of Northern Jutland, Denmark (N-20170047) and conducted in accordance with the Declaration of Helsinki.

Stimulation

Sustained Deep-Tissue Stimulation

A computer-controlled cuff-pressure algometer (CPA) (NociTech, Denmark, and Aalborg University, Denmark) (Polianskis et al. 2002a) was used to deliver pressure stimulation to the right forearm. The CPA consists of a 10-cm wide silicone tourniquet cuff (VBM, Germany), a compressor (Condor MDR2, JUN-AIR International A/S, Nørresundby, Denmark) connected to an electric–pneumatic converter (ITV2030, SMC Corp., Tokyo, Japan) and controlled by a computer through a data acquisition card (PCI 6024E, National Instruments, Austin, TX, USA). The cuff was placed around the right forearm making sure that it was attached over the belly of the extensor carpi radialis brevis (ECRB) muscle 3-cm proximal to the cubital fossa.

Vibrotactile Stimulation

Continuous vibrotactile stimuli (VT) was delivered to the right forearm using a vibrotactile stimulator (g.STIMbox, g.tec medical engineering GmbH, Austria). The vibrotactile was placed under the cuff and over the ECRB muscle, to ensure that the same skin area was stimulated with both modalities. Vibrotactile stimuli consisted of constant-amplitude sinusoidal mechanical vibration delivered at 30 Hz using a vibrotactile transducer (g.VIBROstim, length: 3 cm; width: 1 cm, g.tec medical engineering GmbH, Austria).

Behavioural Data

The participants were instructed to relax, pay attention only to the stimulation and use their left hand to manipulate a slider in a 10-cm visual analogue scale (VAS) device

to score the perceived intensity of each stimulus. Besides, the participant could press a button to stop the stimulation. The intensity of the perceived sensation was rated on a scale anchored from 0 (no sensation at all) to 10 (maximal pain), where 5 represented the pain detection threshold (Hansen et al. 2017). Therefore, VAS scores from 0 to 5 were considered as non-painful, and VAS above 5 up to 10 were regarded as painful. The participants were instructed to start rating the stimulation intensity continuously on the VAS device (sampled at 10 Hz) once the stimulation became noticeable and to press the button to stop the stimulation if the pain became intolerable.

Electrophysiological Data

EEG data were collected using a g.HIamp amplifier (g.tec medical engineering GmbH, Austria) from 64 scalp electrodes placed according to the international 10/20 system. Electrode impedance was kept below 10 kΩ and the sampling rate was 1200 Hz. Electrodes were referenced to the left earlobe (A1) and AFz served as the ground. At the beginning of the experiment, three minutes of eyes-open resting EEG (REEG) recordings were conducted for quality control. To prevent eye movements during resting, the participants were instructed to fix their sight to a fixation cross displayed on the computer screen placed in front of them. Furthermore, to minimize eyes movement during stimulation, participants were instructed to fix their sight to a vertical VAS bar displayed on the computer screen that showed their actual VAS score.

Experimental Setup

Data acquisition was carried out in a single session. Participants were seated on a comfortable chair, with both forearms resting on the armrest and facing a computer screen. Participants wore foam earplugs (Earplugs, TaperFit 3 M, Minnesota, United States) to reduce ambient noise. Prior to the acquisition of data, familiarization trials were conducted to introduce the participants to the cuff pressure sensation and to train them to score with the VAS device. Familiarization trials consisted of the administration of constant stimulation for 2 min at a random pressure that ranged from 10 to 100 kPa. After familiarization, the average of the cuff pressure that elicited VAS 7 and VAS 3 in three consecutive ramps (rate = 1 kPa/s, interstimulus interval = 5 min, pressure limit = 110 kPa) were used to estimate the pressure of the sustained deep-tissue pain (SDTP) and sustained deep-tissue no-pain (SDTnP) conditions, respectively.

The session continued with three stimulation blocks of three minutes each: SDTP, SDTnP, and VT. Both VAS and EEG were recorded simultaneously during stimulation. There was a pause of five minutes between every block, during which no stimulus was presented. The order of the stimulation blocks was randomized across participants. In order to reach the pressure used in the SDTP and SDTnP conditions, the cuff was inflated at a rate of 1 kPa/s until the pressure level was reached, and it was kept constant for three minutes.

EEG Pre-processing

EEG data were exported to Matlab R2016b (The Mathworks Inc, Natick, MA, USA) for off-line processing using EEGLAB toolbox v14.1.1 (Delorme and Makeig 2004). EEG data were digitally band-pass-filtered between 0.1 and 30 Hz and resampled to 500 Hz. The recorded signals were visually inspected to exclude noisy segments (non-cerebral source activity). In the event that a bad/noisy channel was found in a certain participant, such channel was rejected for all conditions for that said participant. A maximum of three channels were removed from the EEG dataset. Moreover, independent component analysis was carried out to remove remaining noise from blinks, muscle activity, and electrode artefacts (Jung et al. 2000). The continuous clean datasets were segmented in 4-s epochs. EEG data length was further reduced to a total of 160 s for each condition to account for differences in the number of segments eliminated during cleaning, ensuring the same amount of data for all the subjects. Furthermore, the first two epochs were rejected to avoid transient evoked responses (Chen et al. 2008). In total, 38 epochs were used in the subsequent analyses per condition and per participant.

Before further data analysis, across-subject grand average scalp topographic of spectral power were plotted for each condition and each frequency band for quality control, since further signal processing steps are highly dependent on artefact-free data (Hoffman 2006). Since eye movements generate increased power in the delta band of the frontal electrodes (Babiloni et al. 2020), this entire frequency range would be disregarded from the analysis in the event that it exhibits clear remnants of artefacts in the delta band topography.

Estimation of Cortical CSD Distribution

For the estimation of the cortical three-dimensional current source density distribution, the exact low-resolution brain electromagnetic tomography (eLORETA) method was used (Pascual-Marqui 2007). The eLORETA (LORETA-KEY software v20150415, http://www.uzh.ch/keyinst/loreta.htm) allows estimating the cortical current density from the EEG

scalp recordings. This is performed by solving the so-called EEG inverse problem (Michel et al. 2004). The solution space is limited to the cortical grey matter and has a volume of 6239 voxels at 5 mm^3 spatial resolution. In this solution, the lead field was computed using a realistic head model based on the Montreal Neurologic Institute average MRI (MNI152) (Lancaster et al. 2000; Fuchs et al. 2002; Brett et al. 2002). The current density was calculated from the cleaned EEG epochs for each condition and for each subject. The eLORETA CSD was estimated for five frequency bands: delta (1–3.9 Hz), theta (4–7.9 Hz), alpha (8–13.9 Hz) and beta (14–29.9 Hz).

The CSD was extracted from seven specific regions of interest (ROIs), which are frequently reported to be active during pain processing (Peyron et al. 2000; Downar et al. 2003; Apkarian et al. 2005; Duerden and Albanese 2013; Jensen et al. 2016), see Table 1. Note that, in the present study, the insulae were the only anatomical regions that were analysed bilaterally. The other selected regions (Table 1) were those located contralateral to the stimulation site. In previous literature, however, some of these areas are reported as being active bilaterally during pain, namely the posterior parietal cortex (PPC), pre-motor cortex (Pre-MC) and dorsolateral-prefrontal cortex (DLPFC). Despite these ipsilateral areas are likely to be active during pain, higher brain activity can be expected in the contralateral counterparts (Shenoy et al. 2011; Yücel et al. 2015). Since the experimental procedure involved the use of the left hand to score their sensation using a VAS, and this task certainly elicits brain activity in the ipsilateral side that could be confounded (Fuchs et al. 2000), it was decided to focus primarily on the contralateral regions, marked with the "L-" (left) prefix throughout the text. The ROIs were defined as the average of all voxels that fell within a 15-mm radius sphere around the seed point (Canuet et al. 2012). Additionally, the absolute CSD of the ROIs during REEG, SDTP, SDTnP and VT was estimated.

Statistical Analysis

Perceived Stimulus Intensity

To assess the effects of the stimulation conditions (SDTP vs. SDTnP vs. VT) on the perceived stimulus intensity, a point-by-point, one-way repeated measures analyses of variance (RM ANOVA) with permutation test (Maris and Oostenveld 2007) was performed on the continuous VAS scores over the 180-s interval using Letswave software (https:// github.com/NOCIONS/letswave6/). The permutation test was performed to control for false positives (type I error) that may result from the multiple comparisons performed for each time point.

CSD Estimations

To assess possible differences in CSD estimations between conditions, a within-subject generalized linear mixed model was built in SPSS (version 24; IBM Corporation, New York, NY). The CSD was defined as the target, while the experimental conditions (three levels: SDTP, SDTnP and VT), the ROIs (seven levels: L-ACC, L-S1, R-AI, L-DLPFC, L-AI, L-PPC, L-S2), the EEG frequencies (three levels: theta, alpha and beta), and all possible combinations between them were included as fixed factors. Furthermore, subject was included as a random effect and the covariance type structure for the residual was specified as compound symmetry. Since the CSD is non-normally distributed (Tzyy-Ping Jung et al. 1997; Cohen 2014), a gamma distribution with a log link was used to fit the model (Bolker et al. 2009). The absolute criterion for parameter convergence of the model was set at $1 \cdot 10^{-5}$. Post-hoc Sidak corrections were applied to adjust for Type I error.

Table 1 Spatial locations of regions of interest considered for the analysis

Side	Region	Abbrev	BA	x	y	z
Left	Anterior cingulate cortex	L-ACC	24	−4	10	30
Left	Primary somatosensory cortex	L-S1	2	−40	−26	48
Right	Anterior insula	R-AI	13	41	13	0
Left	Dorsolateral prefrontal cortex	L-DLPFC	9	−37	17	36
Left	Anterior insula	L-AI	13	−41	13	0
Left	Posterior parietal cortex	L-PPC	7	−18	−62	66
Left	Premotor cortex	L-PreMC	6	−60	1	9

The regions were defined as the average of all voxels that fell within a 15-mm radius sphere around the seed point. Coordinates are in Talairach space

BA Brodmann area, *x* medial–lateral, *y* anterior–posterior, *z* superior-inferior

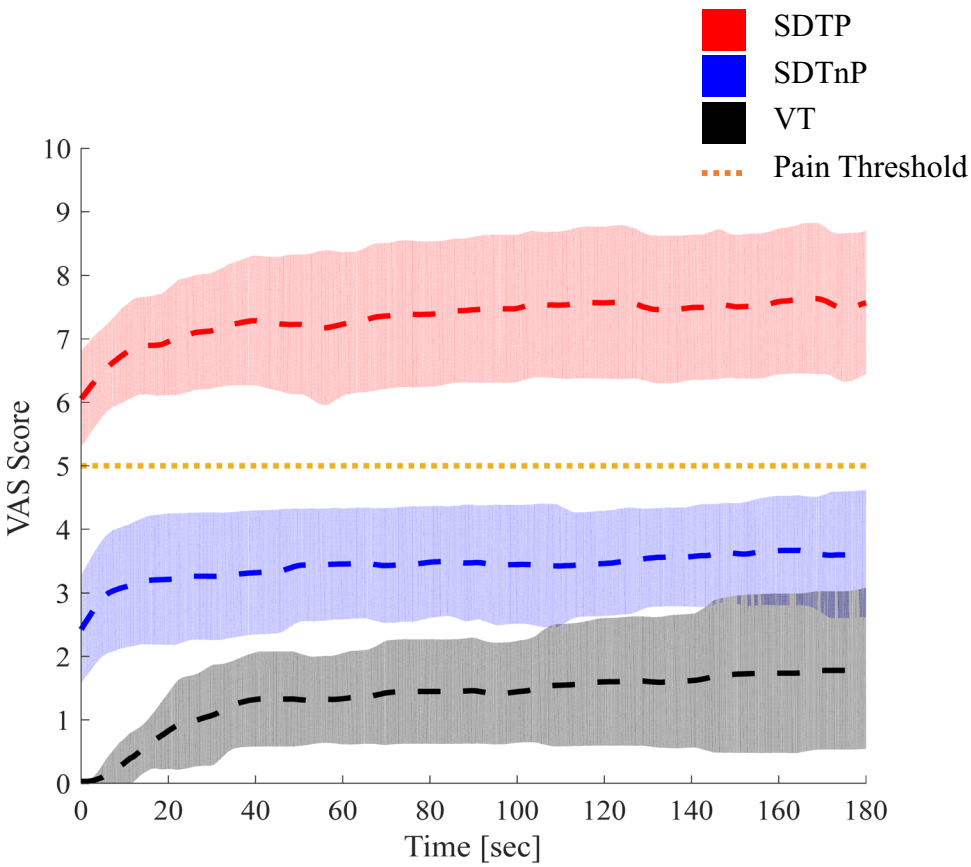

Fig. 1 Mean (dashed) and standard deviation (shaded) visual analogue scale (VAS) scores for all subjects (N = 23) during SDTP (red), SDTnP (blue) and continuous vibrotactile (VT, black) stimulation. Point-by-point, one-way repeated measures analyses of variance with permutation test revealed significant differences across the whole-time interval ($p < 0.001$) in the VAS scores between conditions. The orange dotted line represents the pain threshold anchored at VAS = 5. (red) *SDTP* sustained seep tissue pain, (blue) *SDTnP* sustained deep-tissue no-pain, (black) *VT* continuous vibrotactile (Color figure online)

Results

Perceived Stimulus Intensity

There was a marked difference in the perceived intensity scores between the SDTP, SDTnP, and VT conditions differently across time ($p < 0.001$) in accordance with the intended stimulation levels, see Fig. 1 Neither SDTnP nor VT mean intensity scores surpassed the pain threshold, and the SDTP did not fall below the pain threshold either. Furthermore, the three curves reached a plateau, and habituation was not observed during most of the stimulation period. The mean cuff pressure that elicited SDTnP was 29.69 ± 9.65 kPa and SDTP was 62.02 ± 14.62 kPa.

Topographic Representation

The grand-average scalp topographies for REEG, SDTP, SDTnP and VT for each frequency band are represented in Fig. 2. Higher activity over parieto-occipital electrodes is displayed during REEG in the alpha band, which appears to decrease during stimulation. Moreover, there was higher activity in the frontal electrodes than in the rest of the scalp for the delta band. The estimation of spectral components from frontal electrodes are heavily affected by eye movements (Hagemann and Naumann 2001), and the present scalp maps clearly showed that not all ocular artefacts were separated and rejected from the brain signals. Therefore, the delta band was not included in the statistical analysis.

CSD Estimation

Figure 3 exhibits the current source density of three particular areas (L-ACC, R-AI and L-S1) across the 1–30 Hz frequency range for REEG, SDTP, SDTnP and VT conditions. Overall, the CSD of REEG showed higher values in the delta frequency range in the three regions. Furthermore, a clear peak in the alpha band was observed in S1 during REEG.

The statistical analysis showed a main effect of the condition ($F_{3,1.386} = 99.92$, $p < 0.001$), ROIs ($F_{6,1.386} = 105.19$, $p < 0.001$) and frequency ($F_{2,\ 1.386} = 553.89$, $p < 0.001$) on the CSD. The two-way interactions condition × ROIs ($F_{12,1.386} = 2.11$, $p = 0.014$) and condition × frequency ($F_{6,1.386} = 6.86$, $p < 0.001$) showed significant effect. No effect was found in the tree-way interaction ROIs × condition × frequency ($F_{24,1.386} = 0.67$, $p = 0.885$). Adjusted

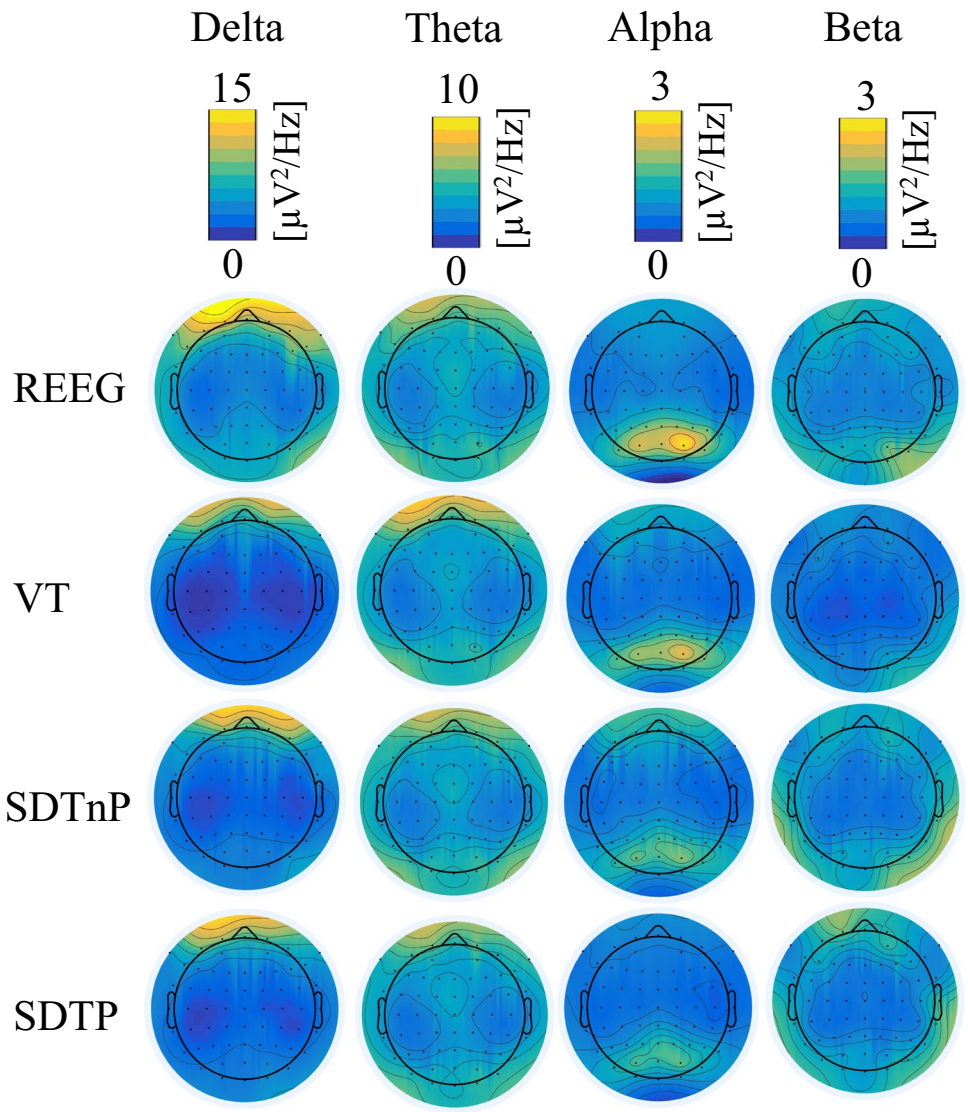

Fig. 2 Grand-average topographic distribution of absolute EEG power across frequency bands and experimental conditions. *REEG* resting EEG, *SDTP* sustained seep tissue pain, *SDTnP* sustained deep-tissue no-pain, *VT* continuous vibrotactile

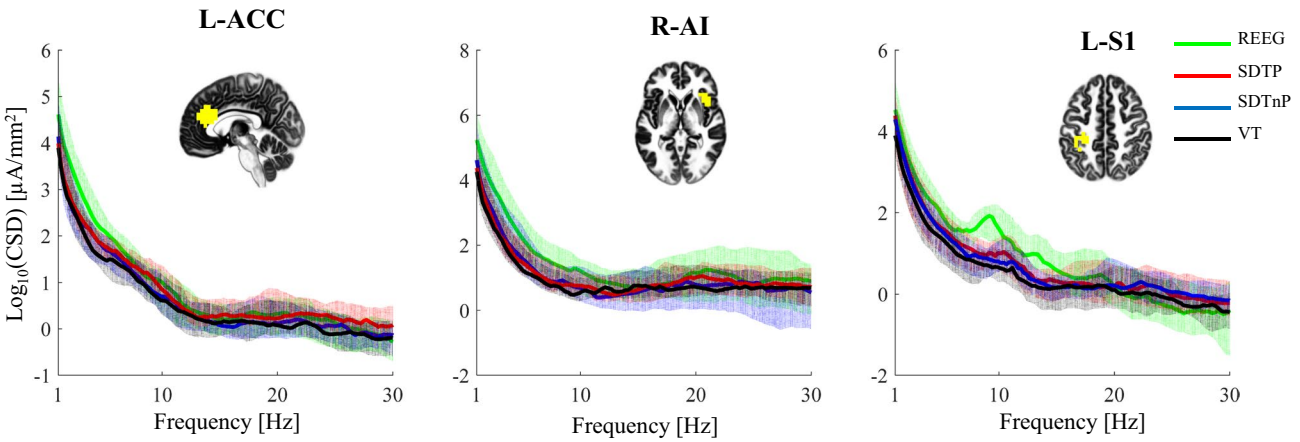

Fig. 3 Across subject mean (±SD) of the Log current source density (CSD) under resting EEG (REEG), sustained deep-tissue pain (SDTP), sustained deep-tissue no-pain (SDTnP) and vibrotactile (VT) of the left anterior cingulate cortex (L-ACC), right anterior insula (R-AI) and left primary somatosensory cortex (L-S1)

Table 2 Pair-wise comparisons of the ROI × condition double interactions

Interaction	ROI × condition		
ROI	Pair-wise	T	p
L-ACC	SDTP–SDTnP	2.40	**0.033**
	SDTP–VT	2.56	**0.032**
	SDTnP–VT	0.16	0.876
L-S1	SDTP–SDTnP	3.41	**0.001**
	SDTP–VT	6.22	**< 0.001**
	SDTnP–VT	2.81	**0.005**
L-AI	SDTP–SDTnP	6.57	**< 0.001**
	SDTP–VT	7.09	**< 0.001**
	SDTnP–VT	0.52	0.605
R-AI	SDTP–SDTnP	4.64	< 0.001
	SDTP–VT	5.13	< 0.001
	SDTnP–VT	0.50	0.619
L-DLPFC	SDTP–SDTnP	4.16	< 0.001
	SDTP–VT	4.38	< 0.001
	SDTnP–VT	0.20	0.826
L-PPC	SDTP–SDTnP	2.59	0.020
	SDTP–VT	2.93	0.010
	SDTnP–VT	0.35	0.729
L-PreMC	SDTP–SDTnP	5.49	< 0.001
	SDTP–VT	6.54	< 0.001
	SDTnP–VT	1.12	0.265

Bold values are significant differences of ($p < 0.05$)

SDTP sustained seep tissue pain, *SDTnP* sustained deep-tissue no-pain, *VT* continuous vibrotactile, *ROIs* regions of interest, *L-ACC* left anterior cingulate cortex, *L-S1* left primary somatosensory cortex, *L-AI* left anterior insula, *R-AI* right anterior insula, *L-DLPFC* left dorsolateral prefrontal cortex, *L-PPC* left posterior parietal cortex, *L-PreMC* left premotor cortex

Table 3 Pair-wise comparisons of the Frequency × condition double interactions

Interaction	Frequency × condition		
ROI	Pair-wise	T	p
Theta	SDTP–SDTnP	8.97	**< 0.001**
	SDTP–VT	11.60	**< 0.001**
	SDTnP–VT	2.64	0.008
Alpha	SDTP–SDTnP	4.13	**< 0.001**
	SDTP–VT	5.73	**< 0.001**
	SDTnP–VT	1.60	**0.106**
Beta	SDTP–SDTnP	6.00	**< 0.001**
	SDTP–VT	5.48	**< 0.001**
	SDTnP–VT	− 0.59	0.598

Bold values are significant differences of ($p < 0.05$)

SDTP sustained seep tissue pain, *SDTnP* sustained deep-tissue no-pain, *VT* continuous vibrotactile

pairwise comparisons of relevant interactions are shown in Tables 2, 3, Fig. 4 and 5.

Analysis of the condition × ROIs interactions showed that the participants presented higher brain activity in the L-ACC, both anterior insulas, the L-DLPFC, L-PPC and L-PreMC when they reported pain (SDTP) compared to when they did not experience pain (SDTnP and VT). Furthermore, the participants had higher activity in the L-S1 for increasing stimulus intensity.

Analysis of the condition × frequency interactions showed that the participants had higher alpha and beta activity when they reported pain compared to when did not. Participants had higher theta activity when increasing the stimulus intensity.

Discussion

The purpose of this study was to characterize the effects of sustained deep-tissue painful stimulation on the brain oscillations in regions involved in pain processing. The results show that evoked activity by painful cuff-pressure algometry can be differentiated from non-painful cuff-pressure algometry. More precisely, increased activity within the L-ACC, AI, L-DLPFC, L-PPC, L-PreMC were consistent with increasingly painful input. In contrast, the activity in L-S1 may be related to somatosensory discrimination of stimulus intensity with higher CSD evoked by pressure algometry in comparison with vibrotactile stimulations.

Stimulus Intensity and Evoked Sensations

In this study, the participants reported steady sensations when the stimulus intensities were held constant. Similarly, previous studies have reported that continuous cuff-pressure algometry and vibrotactile stimulations elicit stable sensations that do not easily adapt or build-up (Polianskis et al. 2002a). This contrasts with other experimental tonic pain models. For instance, intramuscular infusion of hypertonic solution induces temporal summation of pain after its injection, which can last several minutes (Stohler and Kowalski 1999; Arendt-Nielsen and Svensson 2001). Moreover, tonic heat stimulation initially induces temporal summation, in which a non-painful stimulus can become painful (Huber et al. 2006); however, it is followed by pain habituation that may even lead back to non-painful perception (Hashmi and Davis 2009). These adaptive processes certainly modulate the perception of pain and involve different levels of salience (Davis 2011). Thus, conclusions about tonic pain processing and salience can be affected when either habituation or

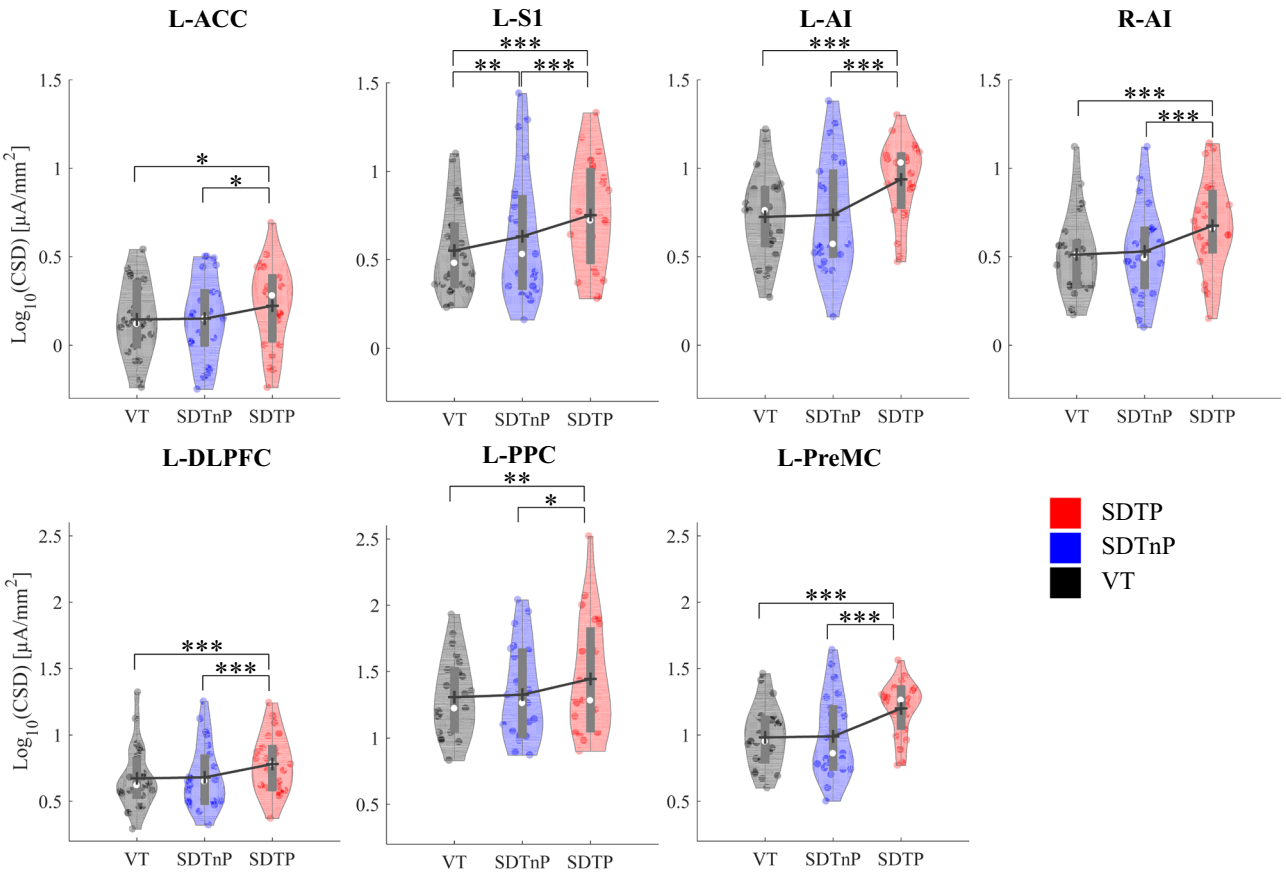

Fig. 4 Violin-plots representing the current source density (CSD) estimations of the interaction between conditions and the regions of interest. The grey bar represents the interquartile range and the white dot the median. The whiskers represent 1.5 times the interquartile range. The outer shape represents the distribution density of the $\log_{10}$(CSD). Each point in the violin represents an individual value. The black line represents the mean of the $\log_{10}$(CSD). *P < 0.05; **P < 0.01; ***P < 0.001. *SDTP* sustained deep-tissue pain, *SDTnP* sustained deep-tissue no-pain, *VT* continuous vibrotactile, *L-ACC* left anterior cingulate cortex, *L-S1* left primary somatosensory cortex, *R-AI* right anterior insula, *L-AI* left anterior insula, *L-DLPFC* left dorsolateral prefrontal cortex, *L-PPC* left posterior parietal cortex, *L-PreMC* left premotor cortex

temporal summation are present (Jepma et al. 2014; Weissman-Fogel et al. 2015). Alternatively, using a stimulus that evokes a constant perception of pain intensity may help to disentangle the mechanisms underlying tonic pain and salience. Consequently, computer-controlled cuff pressure algometry can provide deep stimulation and evoke continuous aching sensation, which consequently decreases the variability in pain ratings associated with the mechanisms previously mentioned (Polianskis et al. 2001).

Effect of Sustained Simulation in the Overall CSD

The present results showed that vibrotactile, sustained deep-tissue painful and non-painful stimulation elicited different activity levels in the studied regions. Particularly, these regions exhibited an overall higher CSD when the participants reported pain in comparison to when they did not feel pain. This is in agreement with several observations that found that self-reported pain intensity strongly correlates with the magnitude of brain oscillations (Tracey and Mantyh 2007; Nir et al. 2012; Zhang et al. 2012; Schulz et al. 2015). These findings are similar to those reported by studies that investigated phasic evoked responses to painful stimulation (Ohara et al. 2004; Iannetti et al. 2005; Zhang et al. 2012), and further supported by neuroimaging evidence (Schneider et al. 2001; Davis et al. 2002; Baliki et al. 2008; Lin et al. 2018).

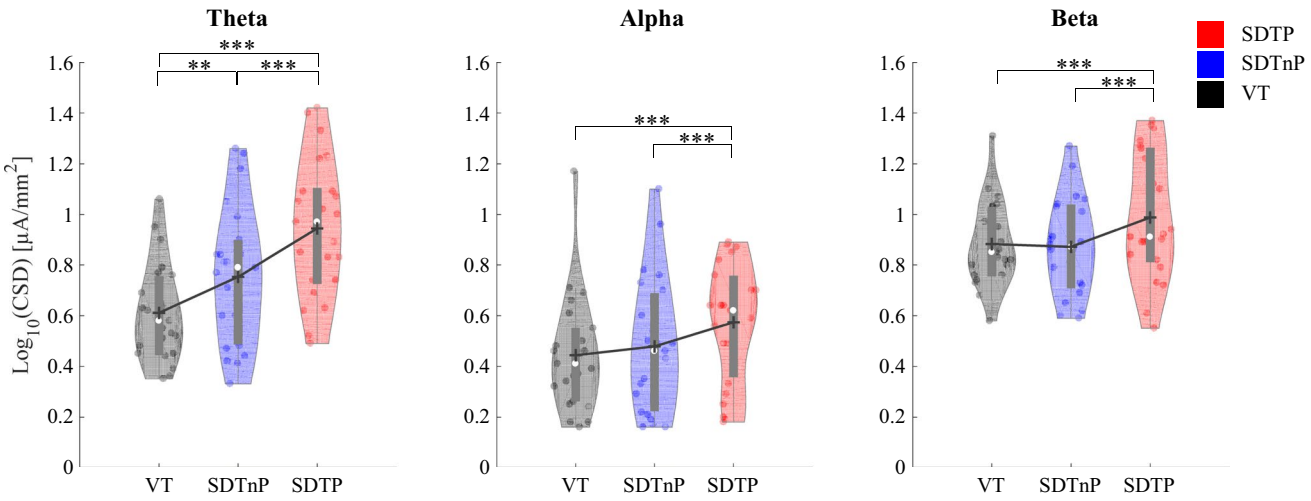

Fig. 5 Violin-plots representing current source density (CSD) estimations of the interaction between conditions and frequency bands. The grey bar represents the interquartile range and the white dot the median. The whiskers represent 1.5 times the interquartile range. The outer shape represents the distribution density of the $\log_{10}$(CSD). Each point in the violin represents an individual value. The black line represents the mean of the $\log_{10}$(CSD). *P < 0.05; **P < 0.01; ***P < 0.001. *SDTP* sustained deep-tissue pain, *SDTnP* sustained deep-tissue no-pain, *VT* continuous vibrotactile

Acute muscle pain serves to protect the body and is subject to an appropriate motor response to avoid further damage and contribute to recovery (Graven-Nielsen 2006). In this experiment, participants continuously slid the VAS scale to quantify the perceived stimulus intensity, which activates sensory and motor cortical areas. Thus, the difference found in the CSD estimations between SDTP and SDTnP may be related to the preparation and the execution of motor responses. Yet, previous evidence suggests that painful and non-painful stimuli do not differ in the influence on motor preparation in the human brain (Postorino et al. 2017). Furthermore, the participants repeated this scoring activity in all three experimental conditions. Therefore, the observed differences in the CSD estimations between conditions cannot be attributed to the scoring task.

During cuff-pressure algometry not only deep-tissue is stimulated, but also the skin. Therefore, differences in CSD estimations between painful and non-painful cuff stimulation may be attributed to factors other than deep pain. However, Polianskis et al. (2002b) induced hyperalgesia in the skin using topical capsaicin cream, yet the participants did not report increased pain sensitivity to cuff stimulation in the treated area. In another study (Manafi-Khanian et al. 2015), the researchers investigated the mechanical stress and strain distribution in superficial and deep tissues during cuff algometry using a computational three-dimensional finite element model of the lower leg; showing that cuff algometry preferentially stimulates deep somatic tissue. On the other hand, vibrotactile stimulation mostly stimulates mechanoreceptors in the skin (Verrillo 1985). Thus, differences in CSD found in this study between cuff pressure and vibrotactile are likely due to different tissues and receptors being stimulated.

The L-ACC and AI are central hubs of a network involved in salience detection called the salience network. Observing brain activity within these regions when a person experiences pain is not sufficient to assume that such activity is a direct correlate of pain perception (Iannetti et al. 2013). A body of work argues that the measured brain activity not only reflects the processing of the perceived stimulus intensity, but it also reflects its salience (Legrain et al. 2003; Iannetti et al. 2008; Wiech et al. 2010). A salient stimulus thus evokes activity in the brain that directs the attention towards any perceived event that may have a potential impact on the organism (Costantini et al. 2008). In other words, a painful experience will generally stand out from other stimuli, since maintaining tissue integrity is crucial. Therefore, the observed increase in brain activity in the most painful condition might not strictly be related to the change in stimulus intensity, but to an increase in the salience of the stimulus (Iannetti et al. 2008; Legrain et al. 2009).

In the present study, each stimulus block lasted three minutes, which highly contrasts to the duration of high-intensity laser or electrical pulses (in the tens of milliseconds) used in the majority of previous studies that investigated the transient brain responses elicited by these stimuli and its functional significance in pain neurophysiology (Legrain et al. 2011). It can be argued that the long-duration, constant stimulation loses its novelty and its ability to capture attention. Still, novelty might not be the only factor that determines the salience of a stimulus, but rather its ability to stand out (Ronga et al. 2013). Indeed, non-painful somatosensory

stimulation requires voluntary attention or behavioural relevance to maintain salience; for instance, voluntary attention to score the perceived sensation continuously on a scale (Frith 2001). On the other hand, constant painful stimulation tends to maintain salience even without voluntary attention, because pain is able to keep attention both involuntarily and continuously (Downar et al. 2003). Therefore, the observed changes in the CSD estimations during SDTP might indeed reflect the processing of the salience of cuff-pressure painful stimulation that makes it stand from the environmental context.

Effect of Sustained Simulation in the ROIs

The present results showed differences in CSD at L-S1 among conditions. It is well documented that S1 is mostly involved in the sensory-discriminative aspects of somatosensory processing, such as stimulus intensity, localization and frequency, (Kenshalo et al. 1988; Jousmäki and Forss 1998; Bushnell et al. 1999). It is worth noting that vibration and pressure are mediated by different receptors. When using a cuff-pressure algometer, the pressure sensation originates from activation of free nerve endings in the deep tissues, conducted via group III (Aδ) and IV (c) afferent fibres that project to S1 via the thalamus (Graven-Nielsen et al. 2004). On the other hand, the vibrotactile sensation originates from activation of Meissner and Pacinian corpuscles in the skin, conducted via group II (Aβ) afferent fibres which also project to S1 (Breitwieser et al. 2012). Furthermore, neuroimaging studies confirm that S1 is not only involved in discriminating the stimulus intensity but also its localization and quality discrimination (Peyron et al. 1999; Hofbauer et al. 2001; Lemus et al. 2010). Therefore, the observed differences in oscillatory activity within S1 between all conditions possibly reflect the differences in somatosensory input given by the different tissue and fibres stimulated by the cuff and vibrotactile stimulator.

CSD in the L-ACC and both AI was higher when the participants reported pain compared to when they did not (SDTnP and VT). Previous researchers have stated that the AI and ACC contribute to a large extent in detecting and attending salient events in the sensory environment (Downar et al. 2002; Wiech et al. 2010). Furthermore, these regions have also been reported to be involved in emotional, sensorimotor, homeostatic and cognitive functions (Bush et al. 2000; Taylor et al. 2009; Dolcos et al. 2011; Gasquoine 2014). The L-DLPFC, L-PPC and L-PreMC exhibited similar responses to the AI and L-ACC. Indeed, previous work indicates that the activation of the PreMC may be associated to the urge of hand withdrawal from the source of pain while the participants were instructed to remain still (Svensson et al. 1997). The activation of PPC is associated with the body awareness of the painful area and sensorimotor coordination (Forss et al. 2005) when compared to non-painful stimulation. Even though the activation of DLPFC has been associated with pain detection (Seminowicz and Davis 2007; Seminowicz and Moayedi 2017), the function of this area during pain is still debated. Except for S1, all the studied areas exhibit a similar increased neuronal activity during sustained deep tissue pain. This supports the notion that none of these regions is exclusive to pain processing but contributes to the different dimensions of pain (Peyron et al. 2000) and their activity is increased under pain.

Last but not least, these results are in accordance with the concept suggested by Davis et al. (2015) where some regions/networks of the brain should work as a "pain switch" that changes its state during pain. In other words, brain oscillations within these regions, seem to be in low activity state ("off") when subjects perceived non-painful stimuli, while it seems to change to high activity state ("on") when subjects perceived pain. However, with the present methods, pain cannot be disentangled from saliency, and therefore further investigations are needed to understand the "pain switch". According to the results of this study, the "pain switch" may not be exclusive of a single region, but a shared trait of several interconnected regions.

EEG Spectral Changes During Sustained Stimulation

Consistent with other studies, increased theta activity was found during tonic pain (Navid et al. 2019). The literature suggests that theta oscillations are related to the level of attention (Fallon et al. 2017; Keller et al. 2017). In the present study, the participants were instructed to keep their attention to the stimulus source and score their perceived sensation across all conditions. Thus, the differences found in CSD in the theta band cannot be only attributed to differences in attention. The present differences were not only observed between painful and non-painful conditions, but also between non-painful stimulations (SDTnP and VT). Even though a few studies have proposed that theta oscillations have an association to pain intensity (Ray et al. 2009; Huishi Zhang et al. 2016), the present findings suggest that theta oscillations in the studied regions may not be exclusively related to pain perception, but rather associated with the amount of somatosensory input.

Increased CSD in the beta band was detected when the participants reported pain. Previous work has observed a desynchronization of the beta band, relative to pre-stimulus activity, immediately after a brief stimulus (Stancák et al. 2003). Another study found that after the desynchronization, there is a beta rebound (Hauck et al. 2007). It is noteworthy, that whereas those studies used repeated brief painful stimulus to test the beta synchronization and desynchronization, the present study applied a constant stimulus, and the first eight seconds of the EEG were excluded. Therefore, it is

unlikely that this beta desynchronization may be reflected in the results. Moreover, beta oscillations are commonly associated with motor functions and increased beta activity is normally observed when a movement has to be resisted or voluntarily suppressed (Androulidakis et al. 2007; Kilavik et al. 2013). The typical defensive response to a painful stimulus is to withdraw the affected limb. In this experimental setting, however, the participants were asked to maintain the forearm in the same position across the experiment. It is therefore likely that the increase in the beta band reflects the voluntary action of suppressing the withdrawal movement (Misra et al. 2017).

The present results showed an increase in the alpha band during SDTP compared to VT and SDTnP. Le Pera and colleagues (2000) also found increased CSD in the alpha band during experimental muscle pain when compared with vibrotactile stimulation. Increased alpha activity has been observed during hand immersion in painful cold water (cold pressor test), compared to immersion in non-painful cool water (Backonja et al. 1991). In the latter, enhanced alpha-band activity was found over central electrodes contralateral to the stimulation site, at the beginning of the painful condition, and followed by a reduction of alpha activity after the first minute. A bulk of work otherwise reported that painful stimulation reduces alpha activity; importantly, these studies compared the painful condition to resting state (Nir et al. 2012; Peng et al. 2014; Hansen et al. 2017; Navid et al. 2019). Current evidence strongly suggests that the alpha band has a functional inhibitory function, i.e., the alpha band activity gates information by inhibiting task-irrelevant regions of the brain (Klimesch et al. 2007; Jensen and Mazaheri 2010). This implies that increased CSD in the alpha band found in the present study may be the consequence of increased cortical inhibition induced by painful cuff-pressure stimulation.

The observed increase in alpha activity during tonic deep-tissue pain may therefore be reflecting a lack of inhibition possibly mediated by the neurotransmitter gamma-aminobutyric acid (GABA) (Klimesch et al. 2007; Başar and Güntekin 2008). Increased GABA levels have been previously measured in the ACC and R-AI with MR spectroscopy during tonic painful stimulation (Jasmin et al. 2005; LaGraize and Fuchs 2007; Kupers et al. 2009). The neurotransmitter GABA is involved in the cortical modulation of pain trough inhibition of synapses in the brain (Olsen and Sieghart 2009). Still, the functional role of the alpha band oscillations in the brain is not fully elucidated (Palva and Palva 2011), and further studies are needed to understand its function in tonic pain processing. The observed differences between power amplitude in the frequency bands are not relevant to discuss; it is well-known that the power spectrum of EEG decays with a ratio of 1/f, resulting in EEG power bands being generally different (Cohen 2017).

Study Considerations and Limitations

Numerous studies have reported an effect of tonic pain in the gamma band (Gross et al. 2007; Schulz et al. 2015; Wang et al. 2016; De Pascalis et al. 2019). Nevertheless, it has been reported that the gamma band is highly contaminated with muscle artefacts (Hipp and Siegel 2013). Indeed, a number of studies showed that scalp EEG high oscillations have an electromyographic origin (Whitham et al. 2007; Yuval-Greenberg et al. 2008). In the last years, several procedures such as phased noise template removal for power line noise, ICA for correcting extra-ocular muscle activity and mathematical modelling to reduce muscle activity, have been applied to obtain only high-frequency brain generated signals (Nottage and Horder 2016). In this study, only visual inspection and ICA were used to eliminate EMG artefacts. Hence, it is not possible to ensure that the origin of the gamma oscillations was only from brain sources.

The present study has some limitations that are important to consider in future studies that investigate the neural correlates of deep-tissue pain. First, this study did not include a stimulus that was salient but non-painful. For instance, this could be achieved by including another sensory modality, e.g. a loud sound, whose salience could be comparable to that of the painful stimulus (Mouraux et al. 2011). This could help elucidate the specificity of the activity within the investigated regions during sustained deep-tissue pain.

Second, eLORETA, which is an improved version of LORETA, was used to estimate the activity in several ROIs involved in pain processing. This technique has been validated and reported as having no localization bias (Pascual-Marqui 2007). Still, the spatial accuracy of eLORETA, like other inverse solution methods, is highly dependent on a number of parameters, e.g. the number and location of electrodes and whether individual MRI data or a template model is being used (Michel et al. 2004; Michel and Brunet 2019).

Third, it is important to highlight that the present findings were mostly related to the contralateral regions, and, to a large extent, the discussion did not consider their laterality during pain. Numerous studies reported that unilateral painful stimulation evokes bilateral activity in a number of regions (Downar et al. 2003), but contralateral regions generally display higher brain activity compared to the ipsilateral counterparts (Shenoy et al. 2011; Yücel et al. 2015). In this experiment, the participants used their left hand to score the ongoing perceived intensity using a VAS device, and brain activity evoked by this action could mask / interact with pain-evoked activity (Fuchs et al. 2000). Hence, considering that this study aimed to identify differences in brain activity between painful and non-painful stimulation conditions, it was decided to focus on the activity of contralateral

regions. Nonetheless, laterality should be considered in future experimental designs.

Finally, 64-channel configuration and a template head model were used to calculate the EEG forward solution and locate the electric brain sources. This approach simplifies the experimental procedure, circumvents the lack of MRI capabilities and avoids the labour-intensive task of measuring the electrode positions on every subject. On the other hand, individual differences in the anatomy of the head and the electrode positions are not taken into account, which can lead to a limited spatial accuracy. Although it is possible to obtain acceptable estimates of the location of the brain sources with these settings, more accurate estimations are obtained when using a whole-head, dense-array sampling (> 256 channels) and the individual MRI of each participant. Due to this constraint, other regions that have been reported to be involved in pain processing (e.g. the primary motor cortex or posterior insula) that are located within a proximity of 3 cm to other regions already included, were disregarded from the analysis (Michel and Brunet 2019). Similarly, deep structures that are important in the endogenous modulation of pain, such as those located in the brainstem, were not included in this analysis. Finally, limiting the number of ROIs is reducing the risk of false positives (type I error).

Conclusions

The present findings indicate that sustained deep tissue pain evokes different responses on brain oscillations compared with innocuous deep tissue stimulation. Results suggest that the increased activity observed among the considered areas between painful and non-painful stimulation (SDTP vs SDTnP and VT) denote physiological differences in neuronal activity that are linked to pain processing. Further studies are required in order to disentangle mechanisms related to pain processing from saliency.

Acknowledgements The Danish National Research Foundation (DNRF121) supports the Center for Neuroplasticity and Pain (CNAP).

References

Androulidakis AG, Doyle LMF, Yarrow K et al (2007) Anticipatory changes in beta synchrony in the human corticospinal system and associated improvements in task performance. Eur J Neurosci 25:3758–3765. https://doi.org/10.1111/j.1460-9568.2007.05620.x

Apkarian AV, Bushnell MC, Treede RD, Zubieta JK (2005) Human brain mechanisms of pain perception and regulation in health and disease. Eur J Pain 9:463–484. https://doi.org/10.1016/j.ejpain.2004.11.001

Arendt-Nielsen L, Svensson P (2001) Referred muscle pain: basic and clinical findings. Clin J Pain 17:11–19. https://doi.org/10.1097/00002508-200103000-00003

Arendt-Nielsen L, Fernández-de-las-Peñas C, Graven-Nielsen T (2011) Basic aspects of musculoskeletal pain: from acute to chronic pain. J Man Manip Ther 19:186–193. https://doi.org/10.1179/106698111X13129729551903

Babiloni C, Barry RJ, Başar E et al (2020) International Federation of Clinical Neurophysiology (IFCN) – EEG research workgroup: Recommendations on frequency and topographic analysis of resting state EEG rhythms. Part 1: applications in clinical research studies. Clin Neurophysiol 131:285–307. https://doi.org/10.1016/j.clinph.2019.06.234

Backonja M, Howland EW, Wang J et al (1991) Tonic changes in alpha power during immersion of the hand in cold water. Electroencephalogr Clin Neurophysiol 79:192–203. https://doi.org/10.1016/0013-4694(91)90137-S

Baliki MN, Geha PY, Apkarian AV (2008) Parsing pain perception between nociceptive representation and magnitude estimation. J Neurophysiol 101:875–887. https://doi.org/10.1152/jn.91100.2008

Başar E, Güntekin B (2008) A review of brain oscillations in cognitive disorders and the role of neurotransmitters. Brain Res 1235:172–193. https://doi.org/10.1016/j.brainres.2008.06.103

Bolker BM, Brooks ME, Clark CJ et al (2009) Generalized linear mixed models: a practical guide for ecology and evolution. Trends Ecol Evol 24:127–135. https://doi.org/10.1016/j.tree.2008.10.008

Breitwieser C, Kaiser V, Neuper C, Müller-Putz GR (2012) Stability and distribution of steady-state somatosensory evoked potentials elicited by vibro-tactile stimulation. Med Biol Eng Comput 50:347–357. https://doi.org/10.1007/s11517-012-0877-9

Brett M, Johnsrude IS, Owen AM (2002) The problem of functional localization in the human brain. Nat Rev Neurosci 3:243–249. https://doi.org/10.1038/nrn756

Bushnell MC, Duncan GH, Hofbauer RK et al (1999) Pain perception: Is there a role for primary somatosensory cortex? Proc Natl Acad Sci 96:7705–7709. https://doi.org/10.1073/pnas.96.14.7705

Bush G, Luu P, Posner MI (2000) Cognitive and emotional influences in anterior cingulate cortex. Trends Cogn Sci 4:215–222. https://doi.org/10.1016/S1364-6613(00)01483-2

Canuet L, Tellado I, Couceiro V et al (2012) Resting-state network disruption and APOE genotype in Alzheimer's disease: a lagged functional connectivity study. PLoS ONE 7:1–12. https://doi.org/10.1371/journal.pone.0046289

Chang PF, Arendt-Nielsen L, Chen ACN (2002) Dynamic changes and spatial correlation of EEG activities during cold pressor test in man. Brain Res Bull 57:667–675. https://doi.org/10.1016/S0361-9230(01)00763-8

Chen ACN, Feng W, Zhao H et al (2008) EEG default mode network in the human brain: spectral regional field powers. Neuroimage 41:561–574. https://doi.org/10.1016/j.neuroimage.2007.12.064

Cohen MX (2014) Analyzing neural time series data

Cohen MX (2017) Where does EEG come from and what does it mean? Trends Neurosci 40:208–218. https://doi.org/10.1016/j.tins.2017.02.004

Costantini M, Galati G, Romani GL, Aglioti SM (2008) Empathic neural reactivity to noxious stimuli delivered to body parts and non-corporeal objects. Eur J Neurosci 28:1222–1230. https://doi.org/10.1111/j.1460-9568.2008.06406.x

Davis KD (2011) Neuroimaging of pain: what does it tell us? Curr Opin Support Palliat Care 5:116–121. https://doi.org/10.1097/SPC.0b013e3283458f96

Davis KD, Pope GE, Crawley AP, Mikulis DJ (2002) Neural correlates of prickle sensation: a percept-related fMRI study. Nat Neurosci 5:1121–1122. https://doi.org/10.1038/nn955

Davis KD, Kucyi A, Moayedi M (2015) The pain switch: an "ouch" detector. Pain 156:2164–2166. https://doi.org/10.1097/j.pain.0000000000000303

Delorme A, Makeig S (2004) EEGLAB: an open sorce toolbox for analysis of single-trail EEG dynamics including independent component anlaysis. J Neurosci Methods 134:9–21. https://doi.org/10.1016/j.jneumeth.2003.10.009

De Pascalis V, Scacchia P, Papi B, Corr PJ (2019) Changes of EEG band oscillations to tonic cold pain and the behavioral inhibition and fight-flight-freeze systems. Personal Neurosci. https://doi.org/10.1017/pen.2019.9

Dolcos F, Iordan AD, Dolcos S (2011) Neural correlates of emotion-cognition interactions: a review of evidence from brain imaging investigations. J Cogn Psychol (Hove) 23:669–694. https://doi.org/10.1080/20445911.2011.594433

Downar J, Crawley AP, Mikulis DJ, Davis KD (2002) A cortical network sensitive to stimulus salience in a neutral behavioral context across multiple sensory modalities. J Neurophysiol 87:615–620. https://doi.org/10.1152/jn.00636.2001

Downar J, Mikulis DJ, Davis KD (2003) Neural correlates of the prolonged salience of painful stimulation. Neuroimage 20:1540–1551. https://doi.org/10.1016/S1053-8119(03)00407-5

Duerden EG, Albanese MC (2013) Localization of pain-related brain activation: a meta-analysis of neuroimaging data. Hum Brain Mapp 34:109–149. https://doi.org/10.1002/hbm.21416

Eccleston C, Crombez G (1999) Pain demands attention: a cognitive–affective model of the interruptive function of pain. Psychol Bull 125:356–366. https://doi.org/10.1037/0033-2909.125.3.356

Fallon N, Chiu Y, Nurmikko T, Stancak A (2017) Altered theta oscillations in resting EEG of fibromyalgia syndrome patients. Eur J Pain. https://doi.org/10.1002/ejp.1076

Forss N, Raij TT, Seppä M, Hari R (2005) Common cortical network for first and second pain. Neuroimage 24:132–142. https://doi.org/10.1016/j.neuroimage.2004.09.032

Frith C (2001) A framework for studying the neural basis of attention. Neuropsychologia 39:1367–1371. https://doi.org/10.1016/S0028-3932(01)00124-5

Fuchs A, Jirsa VK, Kelso JAS (2000) Theory of the relation between human brain activity (MEG) and hand movements. Neuroimage 11:359–369. https://doi.org/10.1006/nimg.1999.0532

Fuchs M, Kastner J, Wagner M et al (2002) A standardized boundary element method volume conductor model integral equation using analytically integrated elements. Clin Neurophysiol 113:702–712. https://doi.org/10.1016/S1388-2457(02)00030-5

Gasquoine PG (2014) Contributions of the insula to cognition and emotion. Neuropsychol Rev 24:77–87. https://doi.org/10.1007/s11065-014-9246-9

Graven-Nielsen T (2006) Fundamentals of muscle pain, referred pain, and deep tissue hyperalgesia. Scand J Rheumatol Suppl 122:1–43. https://doi.org/10.1080/03009740600865980

Graven-Nielsen T, Mense S, Arendt-Nielsen L (2004) Painful and non-painful pressure sensations from human skeletal muscle. Exp Brain Res 159:273–283. https://doi.org/10.1007/s00221-004-1937-7

Gross J, Schnitzler A, Timmermann L, Ploner M (2007) Gamma oscillations in human primary somatosensory cortex reflect pain perception. PLoS Biol 5:1168–1173. https://doi.org/10.1371/journal.pbio.0050133

Hagemann D, Naumann E (2001) The effects of ocular artifacts on (lateralized) broadband power in the EEG. Clin Neurophysiol 112:215–231. https://doi.org/10.1016/S1388-2457(00)00541-1

Hansen TM, Mark EB, Olesen SS et al (2017) Characterization of cortical source generators based on electroencephalography during tonic pain. J Pain Res 10:1401–1409. https://doi.org/10.2147/JPR.S132909

Hashmi JA, Davis KD (2009) Women experience greater heat pain adaptation and habituation than men. Pain 145:350–357. https://doi.org/10.1016/j.pain.2009.07.002

Hauck M, Lorenz J, Engel AK (2007) Attention to painful stimulation enhances γ-band activity and synchronization in human sensorimotor cortex. J Neurosci 27:9270–9277. https://doi.org/10.1523/JNEUROSCI.2283-07.2007

Hipp JF, Siegel M (2013) Dissociating neuronal gamma-band activity from cranial and ocular muscle activity in EEG. Front Hum Neurosci 7:1–11. https://doi.org/10.3389/fnhum.2013.00338

Hofbauer RK, Rainville P, Duncan GH, Bushnell MC (2001) Cortical representation of the sensory dimension of pain. J Neurophysiol 86:402–411. https://doi.org/10.1152/jn.2001.86.1.402

Hoffman DA (2006) LORETA: an attempt at a simple answer to a complex controversy. J Neurother 10:57–72. https://doi.org/10.1300/J184v10n01_05

Huber MT, Bartling J, Pachur D et al (2006) EEG responses to tonic heat pain. Exp Brain Res 173:14–24. https://doi.org/10.1007/s00221-006-0366-1

Huishi Zhang C, Sohrabpour A, Lu Y, He B (2016) Spectral and spatial changes of brain rhythmic activity in response to the sustained thermal pain stimulation. Hum Brain Mapp 37:2976–2991. https://doi.org/10.1002/hbm.23220

Iannetti GD, Zambreanu L, Cruccu G, Tracey I (2005) Operculoinsular cortex encodes pain intensity at the earliest stages of cortical processing as indicated by amplitude of laser-evoked potentials in humans. Neuroscience 131:199–208. https://doi.org/10.1016/j.neuroscience.2004.10.035

Iannetti GD, Hughes NP, Lee MC, Mouraux A (2008) Determinants of laser-evoked EEG responses: pain perception or stimulus saliency? J Neurophysiol 100:815–828. https://doi.org/10.1152/jn.00097.2008

Iannetti GD, Salomons TV, Moayedi M et al (2013) Beyond metaphor: contrasting mechanisms of social and physical pain. Trends Cogn Sci 17:371–378. https://doi.org/10.1016/j.tics.2013.06.002

Jasmin L, Wu M, Ohara P (2005) GABA puts a stop to pain. Curr Drug Target 3:487–505. https://doi.org/10.2174/1568007043336716

Jensen O, Mazaheri A (2010) shaping functional architecture by oscillatory alpha activity: gating by inhibition. Front Hum Neurosci 4:1–8. https://doi.org/10.3389/fnhum.2010.00186

Jensen KB, Regenbogen C, Ohse MC et al (2016) Brain activations during pain: a neuroimaging meta-analysis of patients with pain and healthy controls. Pain 157:1279–1286. https://doi.org/10.1097/j.pain.0000000000000517

Jepma M, Jones M, Wager TD (2014) The dynamics of pain: evidence for simultaneous site-specific habituation and site-nonspecific sensitization in thermal pain. J Pain 15:734–746. https://doi.org/10.1016/j.jpain.2014.02.010

Jousmäki V, Forss N (1998) Effects of stimulus intensity on signals from human somatosensory cortices. NeuroReport 9:3427–3431. https://doi.org/10.1097/00001756-199810260-00017

Jung T-P, Makeig S, Stensmo M, Sejnowski TJ (1997) Estimating alertness from the EEG power spectrum. IEEE Trans Biomed Eng 44:60–69. https://doi.org/10.1109/10.553713

Jung T, Makeig S, Humphries C et al (2000) Removing Electroencephalographic aretfacts by blind source seperation. Psychophysiology 37:163–178. https://doi.org/10.1111/1469-8986.3720163

Kehl LJ, Fairbank CA (2003) Experimental animal models of muscle pain and analgesia. Exerc Sport Sci Rev 31:188–194. https://doi.org/10.1097/00003677-200310000-00006

Keller AS, Payne L, Sekuler R (2017) Characterizing the roles of alpha and theta oscillations in multisensory attention. Neuropsychologia 99:48–63. https://doi.org/10.1016/j.neuropsychologia.2017.02.021

Kenshalo DR, Chudler EH, Anton F, Dubner R (1988) SI nociceptive neurons participate in the encoding process by which monkeys

perceive the intensity of noxious thermal stimulation. Brain Res 454:378–382. https://doi.org/10.1016/0006-8993(88)90841-4
Kilavik BE, Zaepffel M, Brovelli A et al (2013) The ups and downs of beta oscillations in sensorimotor cortex. Exp Neurol 245:15–26. https://doi.org/10.1016/j.expneurol.2012.09.014
Kim J, Loggia ML, Edwards RR et al (2013) Sustained deep-tissue pain alters functional brain connectivity. Pain 154:1343–1351. https://doi.org/10.1016/j.pain.2013.04.016
Klimesch W, Sauseng P, Hanslmayr S (2007) EEG alpha oscillations: The inhibition-timing hypothesis. Brain Res Rev 53:63–88. https://doi.org/10.1016/j.brainresrev.2006.06.003
Kupers RC, Svensson P, Jensen TS (2004) Central representation of muscle pain and mechanical hyperesthesia in the orofacial region: a positron emission tomography study. Pain 108:284–293. https://doi.org/10.1016/j.pain.2003.12.029
Kupers R, Danielsen ER, Kehlet H et al (2009) Painful tonic heat stimulation induces GABA accumulation in the prefrontal cortex in man. Pain 142:89–93. https://doi.org/10.1016/j.pain.2008.12.008
LaGraize SC, Fuchs PN (2007) GABAA but not GABAB receptors in the rostral anterior cingulate cortex selectively modulate pain-induced escape/avoidance behavior. Exp Neurol 204:182–194. https://doi.org/10.1016/j.expneurol.2006.10.007
Lancaster JL, Woldorff MG, Parsons LM et al (2000) Automated Talairach Atlas labels for functional brain mapping. Hum Brain Mapp 10:120–131. https://doi.org/10.1002/1097-0193(200007)10:3%3c120::AID-HBM30%3e3.0.CO;2-8
Lavigne G, Brousseau M, Kato T et al (2004) Experimental pain perception remains equally active over all sleep stages. Pain 110:646–655. https://doi.org/10.1016/j.pain.2004.05.003
Legrain V, Bruyer R, Guérit J-M, Plaghki L (2003) Nociceptive processing in the human brain of infrequent task-relevant and task-irrelevant noxious stimuli. A study with event-related potentials evoked by CO_2 laser radiant heat stimuli. Pain 103:237–248
Legrain V, Perchet C, García-Larrea L (2009) Involuntary orienting of attention to nociceptive events: neural and behavioral signatures. J Neurophysiol 102:2423–2434. https://doi.org/10.1152/jn.00372.2009
Legrain V, Iannetti GD, Plaghki L, Mouraux A (2011) The pain matrix reloaded: a salience detection system for the body. Prog Neurobiol 93:111–124. https://doi.org/10.1016/j.pneurobio.2010.10.005
Lemus L, Hernández A, Luna R et al (2010) Do sensory cortices process more than one sensory modality during perceptual judgments? Neuron 67:335–348. https://doi.org/10.1016/j.neuron.2010.06.015
Le Pera D, Svensson P, Valeriani M et al (2000) Long-lasting effect evoked by tonic muscle pain on parietal EEG activity in humans. Clin Neurophysiol 111:2130–2137. https://doi.org/10.1016/S1388-2457(00)00474-0
Lin Q, Li L, Liu J et al (2018) Influence of individual differences in fMRI-based pain prediction models on between-individual prediction performance. Front Neurosci 12:1–12. https://doi.org/10.3389/fnins.2018.00569
Manafi-Khanian B, Arendt-Nielsen L, Frøkjær JB, Graven-Nielsen T (2015) Deformation and pressure propagation in deep somatic tissue during painful cuff algometry. Eur J Pain (United Kingdom) 19:1456–1466. https://doi.org/10.1002/ejp.677
Maris E, Oostenveld R (2007) Nonparametric statistical testing of EEG- and MEG-data. J Neurosci Methods 164:177–190. https://doi.org/10.1016/j.jneumeth.2007.03.024
Michel CM, Brunet D (2019) EEG source imaging: a practical review of the analysis steps. Front Neurol. https://doi.org/10.3389/fneur.2019.00325
Michel CM, Murray MM (2012) Towards the utilization of EEG as a brain imaging tool. Neuroimage 61:371–385. https://doi.org/10.1016/j.neuroimage.2011.12.039
Michel CM, Murray MM, Lantz G et al (2004) EEG source imaging. Clin Neurophysiol 115:2195–2222. https://doi.org/10.1016/j.clinph.2004.06.001
Misra G, Ofori E, Chung JW, Coombes SA (2017) Pain-related suppression of beta oscillations facilitates voluntary movement. Cereb Cortex 27:2592–2606. https://doi.org/10.1093/cercor/bhw061
Mouraux A, Diukova A, Lee MC et al (2011) A multisensory investigation of the functional significance of the "pain matrix." Neuroimage 54:2237–2249. https://doi.org/10.1016/j.neuroimage.2010.09.084
Navid MS, Lelic D, Niazi IK et al (2019) The effects of chiropractic spinal manipulation on central processing of tonic pain—a pilot study using standardized low-resolution brain electromagnetic tomography (sLORETA). Sci Rep 9:6925. https://doi.org/10.1038/s41598-019-42984-3
Nir RR, Sinai A, Moont R et al (2012) Tonic pain and continuous EEG: Prediction of subjective pain perception by alpha-1 power during stimulation and at rest. Clin Neurophysiol 123:605–612. https://doi.org/10.1016/j.clinph.2011.08.006
Nottage JF, Horder J (2016) State-of-the-art analysis of high-frequency (gamma range) electroencephalography in humans. Neuropsychobiology 72:219–228. https://doi.org/10.1159/000382023
Ohara S, Crone NE, Weiss N et al (2004) Amplitudes of laser evoked potential recorded from primary somatosensory, parasylvian and medial frontal cortex are graded with stimulus intensity. Pain 110:318–328. https://doi.org/10.1016/j.pain.2004.04.009
Olsen RW, Sieghart W (2009) GABA A receptors: subtypes provide diversity of function and pharmacology. Neuropharmacology 56:141–148. https://doi.org/10.1016/j.neuropharm.2008.07.045
Palva S, Palva JM (2011) Functional roles of alpha-band phase synchronization in local and large-scale cortical networks. Front Psychol 2:1–15. https://doi.org/10.3389/fpsyg.2011.00204
Pascual-Marqui RD (2007) Discrete, 3D distributed, linear imaging methods of electric neuronal activity. Part 1: exact, zero error localization. Neurosci Lett 485:198–203. https://doi.org/10.1016/j.neulet.2010.09.011
Peng W, Hu L, Zhang Z, Hu Y (2014) Changes of spontaneous oscillatory activity to tonic heat pain. PLoS ONE 9:1–11. https://doi.org/10.1371/journal.pone.0091052
Peyron R, García-Larrea L, Grégoire M-C et al (1999) Haemodynamic brain responses to acute pain in humans. Brain 122:1765–1780. https://doi.org/10.1093/brain/122.9.1765
Peyron R, Laurent B, García-Larrea L (2000) Functional imaging of brain responses to pain. A review and meta-analysis (2000). Neurophysiol Clin Neurophysiol 30:263–288. https://doi.org/10.1016/S0987-7053(00)00227-6
Ploner M, Sorg C, Gross J (2017) Brain rhythms of pain. Trends Cogn Sci 21:100–110. https://doi.org/10.1016/j.tics.2016.12.001
Polianskis R, Graven-Nielsen T, Arendt-Nielsen L (2001) Computer-controlled pneumatic pressure algometry—a new technique for quantitative sensory testing. Eur J Pain 5:267–277. https://doi.org/10.1053/eujp.2001.0245
Polianskis R, Graven-Nielsen T, Arendt-Nielsen L (2002a) Spatial and temporal aspects of deep tissue pain assessed by cuff algometry. Pain 100:19–26. https://doi.org/10.1016/S0304-3959(02)00162-8
Polianskis R, Graven-Nielsen T, Arendt-Nielsen L (2002b) Pressure-pain function in desensitized and hypersensitized muscle and skin assessed by cuff algometry. J Pain 3:28–37. https://doi.org/10.1054/jpai.2002.27140
Postorino M, May ES, Nickel MM et al (2017) Influence of pain on motor preparation in the human brain. J Neurophysiol 118:2267–2274. https://doi.org/10.1152/jn.00489.2017
Ray NJ, Jenkinson N, Kringelbach ML et al (2009) Abnormal thalamocortical dynamics may be altered by deep brain stimulation: using

magnetoencephalography to study phantom limb pain. J Clin Neurosci 16:32–36. https://doi.org/10.1016/j.jocn.2008.03.004
Ritter P, Villringer A (2006) Simultaneous EEG-fMRI. Neurosci Biobehav Rev 30:823–838. https://doi.org/10.1016/j.neubiorev.2006.06.008
Ronga I, Valentini E, Mouraux A, Iannetti GD (2013) Novelty is not enough: laser-evoked potentials are determined by stimulus saliency, not absolute novelty. J Neurophysiol 44:692–701. https://doi.org/10.1152/jn.00464.2012
Schneider F, Habel U, Holthusen H et al (2001) Subjective ratings of pain correlate with subcortical-limbic blood flow: an fMRI study. Neuropsychobiology 43:175–185. https://doi.org/10.1159/000054887
Schulz E, May ES, Postorino M et al (2015) Prefrontal gamma oscillations encode tonic pain in humans. Cereb Cortex 25:4407–4414. https://doi.org/10.1093/cercor/bhv043
Seminowicz D, Davis KD (2007) Pain enhances functional connectivity of a brain network evoked by performance of a cognitive task. J Neurophysiol 97:3651–3659. https://doi.org/10.1152/jn.01210.2006
Seminowicz DA, Moayedi M (2017) The dorsolateral prefrontal cortex in acute and chronic pain. J Pain 18:1027–1035. https://doi.org/10.1016/j.jpain.2017.03.008
Shenoy R, Roberts K, Papadaki A et al (2011) Functional MRI brain imaging studies using the Contact Heat Evoked Potential Stimulator (CHEPS) in a human volunteer topical capsaicin pain model. J Pain Res 4:365–371. https://doi.org/10.2147/JPR.S24810
Soares JJF, Jablonska B (2004) Psychosocial experiences among primary care patients with and without musculoskeletal pain. Eur J Pain 8:79–89. https://doi.org/10.1016/S1090-3801(03)00083-1
Stancák A, Svoboda J, Rachmanová R et al (2003) Desynchronization of cortical rhythms following cutaneous stimulation: effects of stimulus repetition and intensity, and of the size of corpus callosum. Clin Neurophysiol 114:1936–1947. https://doi.org/10.1016/S1388-2457(03)00201-3
Stohler CS, Kowalski CJ (1999) Spatial and temporal summation of sensory and affective dimensions of deep somatic pain. Pain 79:165–173. https://doi.org/10.1016/S0304-3959(98)00171-7
Svensson P, Arendt-Nielsen L (1995) Induction and assessment of experimental muscle pain. J Electromyogr Kinesiol 5:131–140. https://doi.org/10.1016/1050-6411(95)00019-V
Svensson P, Minoshima S, Beydoun A et al (1997) Cerebral processing of acute skin and muscle pain in humans. J Neurophysiol 78:450–460. https://doi.org/10.1152/jn.1997.78.1.450
Taylor KS, Seminowicz DA, Davis KD (2009) Two systems of resting state connectivity between the insula and cingulate cortex. Hum Brain Mapp 30:2731–2745. https://doi.org/10.1002/hbm.20705
Thunberg J, Lyskov E, Korotkov A et al (2005) Brain processing of tonic muscle pain induced by infusion of hypertonic saline. Eur J Pain 9:185–194. https://doi.org/10.1016/j.ejpain.2004.05.003
Tracey I, Mantyh PW (2007) The cerebral signature for pain perception and its modulation. Neuron 55:377–391. https://doi.org/10.1016/j.neuron.2007.07.012
Verrillo RT (1985) Psychophysics of vibrotactile stimulation. J Acoust Soc Am 77:225–232. https://doi.org/10.1121/1.392263
Wang L, Gui P, Li L et al (2016) Neural correlates of heat-evoked pain memory in humans. J Neurophysiol 115:1596–1604. https://doi.org/10.1152/jn.00126.2015
Weissman-Fogel I, Dror A, Defrin R (2015) Temporal and spatial aspects of experimental tonic pain: understanding pain adaptation and intensification. Eur J Pain (United Kingdom) 19:408–418. https://doi.org/10.1002/ejp.562
Whitham EM, Pope KJ, Fitzgibbon SP et al (2007) Scalp electrical recording during paralysis: quantitative evidence that EEG frequencies above 20 Hz are contaminated by EMG. Clin Neurophysiol 118:1877–1888. https://doi.org/10.1016/j.clinph.2007.04.027
Wiech K, Lin C, Brodersen KH et al (2010) Anterior insula integrates information about salience into perceptual decisions about pain. J Neurosci 30:16324–16331. https://doi.org/10.1523/JNEUROSCI.2087-10.2010
Yücel MA, Aasted CM, Petkov MP et al (2015) Specificity of hemodynamic brain responses to painful stimuli: a functional near-infrared spectroscopy study. Sci Rep 5:1–9. https://doi.org/10.1038/srep09469
Yuval-Greenberg S, Tomer O, Keren AS et al (2008) Transient induced gamma-band response in EEG as a manifestation of miniature saccades. Neuron 58:429–441. https://doi.org/10.1016/j.neuron.2008.03.027
Zhang ZG, Hu L, Hung YS et al (2012) Gamma-band oscillations in the primary somatosensory cortex–a direct and obligatory correlate of subjective pain intensity. J Neurosci 32:7429–7438. https://doi.org/10.1523/jneurosci.5877-11.2012